Synthesis, characterization and photophysics of polyplatinaynes based on bis(9,9-dibutyl-2,7-fluorenyl)-2,1,3-benzothiadiazole derivatives

Qiwei Wang[a,b]*, Lu Jiang[a], Wai-Yeung Wong[b,c]**

[a] *Antibiotics Research and Reevaluation Key Laboratory of Sichuan Province, Sichuan Industrial Institute of Antibiotics, Chengdu University, Chengdu 610052, PR China*

[b] *Department of Chemistry, Hong Kong Baptist University, Kowloon Tong, Hong Kong, PR China*

[c] *Department of Applied Biology and Chemical Technology, The Hong Kong Polytechnic University, Hung Hom, Hong Kong, PR China*

Dedicated to the JOM 1000 Special Issue

* Corresponding author. Antibiotics Research and Reevaluation Key Laboratory of Sichuan Province, Sichuan Industrial Institute of Antibiotics, Chengdu University, Chengdu 610052, PR China.
** Corresponding author. Department of Applied Biology and Chemical Technology, The Hong Kong Polytechnic University, Hung Hom, Hong Kong, PR China.
    E-mail addresses: wqw@cioc.ac.cn (W.-Q.W.), wai-yeung.wong@polyu.edu.hk (W.-Y. Wong)

Abstract: 2,1,3-Benzothiadiazole (BT) and its derivatives are very important acceptor units used in the development of photofunctional compounds and are applicable for the molecular construction of organic optoelectronic devices. Due to their strong electron-withdrawing ability, construction of molecules with the unit core of BT and its derivatives can usually improve the electronic properties of the resulting organic materials. New organometallic acetylide polymers of platinum(II) bridged by bis(fluorenyl)-benzothiadiazole moiety **P1** and **P2** have been synthesized via the CuI-catalyzed dehydrohalogenation reaction of the platinum(II) chloride precursors and the corresponding diacetylene ligands. The photophysical, thermal and electrochemical properties of **P1** and **P2** were investigated.

Keywords: Acetylide; Benzothiadiazole; Fluorene; Metallopolymer; Platinum

1. Introduction

π-Conjugated compounds are important in the building up of organic optoelectronic materials due to their ability to precisely tune the optoelectric properties, such as conductivity, charge-carrier mobility, light absorption and light emission [1, 2]. As a consequence, scientists have made great efforts to design organic compounds with excellent charge transport properties. Among the developed organic optoelectronic π-conjugated molecules, the deployment of donor (D)-acceptor (A) structures is one of the most effective strategies to modulate the optoelectronic properties of these materials [3–5]. Their band gap levels and optoelectronic properties can be easily tuned through systematic variation between the D and A units [6]. Furthermore, hybridization of the energy levels between the D and A units can decrease the highest occupied molecular orbital (HOMO) and the lowest unoccupied molecular orbital (LUMO) energy levels, which results in a rather narrow HOMO-LUMO energy separation [7]. Therefore, the selection of D and A units is particularly important to design and synthesize organic π-conjugated materials with outstanding optoelectronic traits.

Aromatic heterocycles with high HOMO energy levels (E_{HOMO}) have received much attention as strong and synthetically accessible acceptors. A variety of heterocyclic acceptors have been investigated [8–13]. Among these, 2,1,3-benzothiadiazole (BT) [14–18] and its derivatives are promising types of acceptor units, owing to their strong electron-withdrawing property, intense light absorption and good photochemical stability, and are often coupled with a variety of

electron-rich groups to form low-bandgap polymers, small molecules and transition metal complexes [14, 17, 19–23]. They were also employed as electron-transport materials, and have been widely incorporated into polyfluorene-based copolymers to alter the energy levels and fine-tune the emission color over the entire visible region [24]. Recently, a series of fluorene-benzothiadiazole containing polymers have been synthesized and widely used in organic solar cells [25]. In spite of the high hole mobility and weak electron-transport nature of polyfluorene, alternating fluorene-benzothiadiazole containing polymer exhibits a reduced LUMO level and hence enhanced electron mobility due to the high content of electron-deficient benzothiadiazole units. BT derivatives have been applied in various fields such as organic photovoltaics (OPVs), dye-sensitized solar cells (DSSCs), organic field-effect transistors (OFETs), organic light-emitting diodes (OLEDs), and electrochromic devices (ECDs) [3–5].

Here, two new bis(fluorenyl)-benzothiadiazole containing platinum polymers **P1**-**P2** were designed and synthesized (Fig. 1). The solubility of fluorene polymers was tuned by introducing alkyl groups and the π-electron conjugation length of polymer main chain could be extended by adding the thiophene ring with the aim of improving their absorption properties. Investigations of the photophysical, thermal and electrochemical properties of these platinum(II)-containing polyyne polymers were conducted and the absorption/emission data were compared with their discrete model complexes **M1**−**M2**.
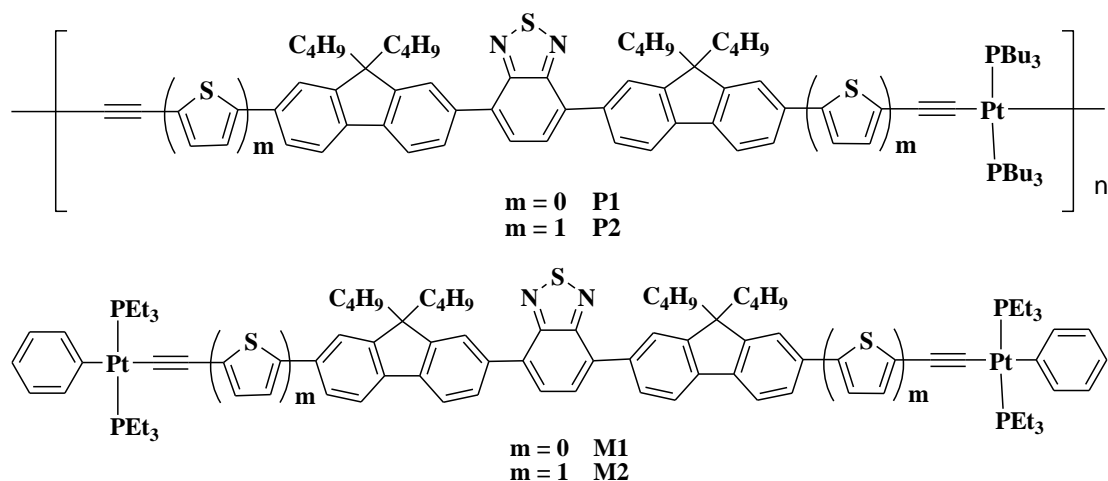
Fig. 1. Chemical structures of fluorene-benzothiadiazole containing Pt(II) polymers **P1**–**P2** and their model complexes **M1**–**M2**.

2.   Experimental section

2.1. *Materials and general experimental*

All reactions were carried out under a nitrogen atmosphere by using standard Schlenk techniques. Solvents were dried and distilled from appropriate drying agents under an inert atmosphere prior to use. All reagents and chemicals, unless otherwise stated, were purchased from commercial sources and used without further purification. *trans*-Pt(PEt$_3$)$_2$(Ph)Cl [26] and *trans*-Pt(PBu$_3$)$_2$Cl$_2$ [27] were prepared according to the literature methods. All reactions were monitored by thin-layer chromatography (TLC) with Merck pre-coated glass plates. Flash column chromatography and preparative TLC were carried out using silica gel from Merck (230–400 mesh).

Infrared spectra were recorded as dichloromethane (CH$_2$Cl$_2$) solutions using a Perkin-Elmer Paragon 1000 PC or Nicolet Magna 550 Series II FT-IR spectrometer, using CaF$_2$ cells with a 0.5 mm path length. Fast atom bombardment (FAB) mass

spectra were recorded on a Finnigan MAT SSQ710 system and MALDI-TOF (matrix-assisted laser desorption/ionization time-of-flight) spectra were obtained by a Autoflex Bruker MALDI-TOF mass spectrometer. NMR spectra were measured in $CDCl_3$ on a Varian Inova 400 MHz FT-NMR spectrometer and chemical shifts are quoted relative to tetramethylsilane for ^1H and ^{13}C nuclei and H_3PO_4 for ^{31}P nucleus.

The cyclic voltammograms were acquired with a CHI model 600D electrochemistry station in deoxygenated acetonitrile containing 0.1 M [Bu$_4$N]PF$_6$ as the supporting electrolyte. A conventional three-electrode configuration consisting of a platinum working electrode, a Pt-wire counter electrode and a Ag/AgCl reference electrode was used. The polymer films were casted on the ITO covered glass. All potentials reported were quoted with reference to the ferrocene-ferrocenium (Fc/Fc$^+$) couple at a scan rate of 100 mV s^{-1}.

2.2. Crystal structures of compounds L1-TMS and 3

Crystals of **L1-TMS** and **3** suitable for X-ray diffraction studies were grown by slow evaporation of their respective solutions in *n*-hexane/CH$_2$Cl$_2$ at room temperature. Geometric and intensity data were collected using graphite-monochromated Mo-K$_\alpha$ radiation ($\lambda = 0.71073$ Å) on a Bruker AXS SMART 1000 CCD area-detector. Cell parameters and orientation matrix for all crystal samples were obtained from the least-squares refinement of reflections measured in three different sets of 15 frames each. The collected frames were processed with the software SAINT [28] and an absorption correction was applied (SDABS) [29] to the

collected reflections. The space groups of each crystal were determined from the systematic absences and Laue symmetry check and confirmed by successful refinement of the structure. The structures of these molecules were solved by direct methods (SHELXTL) in conjunction with standard difference Fourier techniques and subsequently refined by full-matrix least-squares analyses on F^2. All non-hydrogen atoms were assigned with anisotropic displacement parameters. In all cases, the hydrogen atoms on the aromatic rings were generated in their idealized positions and allowed to ride on the respective carbon atoms. The crystallographic parameters, data collection and structure refinement details are summarized in Table 1. CCDC-2288832 to 2288833 contain the supplementary crystallographic data for this paper. These data can be obtained free of charge from the Cambridge Crystallographic Data Centre via www.ccdc.cam.ac.uk/data_request/cif.

2.3. Synthesis

*2.3.1. Synthesis of **L1-I***

To a 100 mL round-bottom flask containing a mixture of Pd(PPh$_3$)$_4$ (72 mg) and 4,7-dibromo-2,1,3-benzothiadiazole (459 mg, 1.56 mmol) in toluene (70 mL), 9,9-bis(*n*-butyl)-2-(tributylstannyl)fluorene (3.10 g, 5.47 mmol) [30] was then added. The mixture was heated to reflux for 24 h under a nitrogen atmosphere. The solution was then allowed to cool to room temperature and the solvents were removed on a rotary evaporator *in vacuo*. The crude product was purified by column chromatography on silica gel eluting with hexane/CH$_2$Cl$_2$ (4:1, v/v) as eluent to provide 4,7-bis(9,9-dibutylfluoren-2-yl)-2,1,3-benzothiadiazole (compound **2**, 804 mg,

1.17 mmol, 75%) as a yellow solid.

Spectral Data: ^{1}H NMR (400 MHz, CDCl$_3$): δ = 8.05−8.03 (m, 2H, Ar), 7.95 (m, 2H, Ar), 7.90−7.87 (m, 4H, Ar), 7.79−7.77 (m, 2H, Ar), 7.40−7.34 (m, 6H, Ar), 2.09−2.02 (m, 4H, C$_4$H$_9$), 1.15−1.10 (m, 8H, C$_4$H$_9$), 0.78−0.70 (m, 20H, C$_4$H$_9$) ppm. ^{13}C NMR (100 MHz, CDCl$_3$): δ = 154.35, 151.28, 151.11, 141.34, 140.67, 136.20, 133.58, 128.16, 127.92, 127.27, 126.85, 123.84, 122.97, 119.95, 119.70 (Ar), 55.14 (quat. C), 40.14, 26.08, 23.12, 13.85 (C$_4$H$_9$) ppm. FAB-MS (*m/z*): 688.5 [M+1]$^+$.

A mixture of **2** (804 mg, 1.17 mmol), iodine (423 mg, 1.64 mmol), periodic acid (293 mg, 1.29 mmol), solvents (concentrated sulfuric acid/water/glacial acetic acid = 2.3 mL/7.7 mL/74 mL, 40 mL) and CCl$_4$ (30 mL) was stirred at 80 °C overnight. After cooling to room temperature, the solution was poured into ice-cooled water containing a large amount of sodium sulfite and the resulting mixture was extracted with dichloromethane (40 mL) twice. The combined organic phases were washed with water (40 mL) twice, dried over anhydrous Na$_2$SO$_4$ and concentrated to dryness. The crude product was purified by column chromatography on silica gel eluting with hexane/CH$_2$Cl$_2$ (2:1, v/v) to provide **L1**-**I** (568 mg, 0.60 mmol, 51%) as a yellow solid.

Spectral Data: ^{1}H NMR (400 MHz, CDCl$_3$): δ = 8.04−8.02 (m, 2H, Ar), 7.93 (m, 2H, Ar), 7.88 (m, 2H, Ar), 7.85−7.83 (m, 2H, Ar), 7.72−7.69 (m, 4H, Ar), 7.53−7.51 (m, 2H, Ar), 2.10−1.94 (m, 8H, C$_4$H$_9$), 1.16−1.10 (m, 8H, C$_4$H$_9$), 0.74−0.71 (m, 20H, C$_4$H$_9$) ppm. ^{13}C NMR (100 MHz, CDCl$_3$): δ = 154.27, 153.69, 150.57, 140.32, 140.31,

8

136.81, 136.00, 133.52, 132.18, 129.05, 128.37, 128.24, 127.97, 125.31, 123.85, 121.69, 119.89, 92.92 (Ar), 55.44 (quat. C), 40.02, 26.04, 23.07, 13.85 (C_4H_9) ppm. FAB-MS (*m/z*): 940.3 [M+1]$^+$.

2.3.2. Synthesis of *L2-Br*

To a 100 mL round-bottom flask was added a mixture of Pd(PPh$_3$)$_4$ (47 mg) and **L1**-**I** (568 mg, 0.60 mmol) in toluene (50 mL) and (tributylstannyl)thiophene (789 mg, 2.11 mmol) was then added. The mixture was heated to reflux for 24 h under a nitrogen atmosphere. The solution was then allowed to cool to room temperature and the solvents were removed on a rotary evaporator *in vacuo*. The crude product was purified by column chromatography on silica gel eluting with hexane/CH$_2$Cl$_2$ (4:1, v/v) to provide 4,7-bis(7-(thiophen-2-yl)-9,9-dibutylfluoren-2-yl)- 2,1,3-benzothiadiazole (compound **3**, 224 mg, 0.26 mmol, 44%) as a yellow solid.

Spectral Data: ^{1}H NMR (400 MHz, CDCl$_3$): δ = 8.07−8.04 (m, 2H, Ar), 7.96 (m, 2H, Ar), 7.91−7.87 (m, 4H, Ar), 7.78−7.76 (m, 2H, Ar), 7.66−7.62 (m, 4H, Ar), 7.42 (m, 2H, Ar), 7.32−7.30 (m, 2H, Ar), 7.14−7.12 (m, 2H, Ar), 2.12−2.06 (m, 8H, C_4H_9), 1.15−1.11 (m, 8H, C_4H_9), 0.81−0.71 (m, 20H, C_4H_9) ppm. ^{13}C NMR (100 MHz, CDCl$_3$): δ = 154.34, 152.11, 151.31, 145.15, 140.87, 140.24, 136.29, 133.55, 133.46, 128.30, 128.09, 127.93, 125.04, 124.60, 123.87, 122.97, 120.36, 120.26, 119.76 (Ar), 55.29 (quat. C), 40.17, 26.10, 23.11, 13.85 (C_4H_9) ppm. FAB-MS (*m/z*): 852.5 [M+1]$^+$.

Compound **3** (214, 0.25 mmol) was dissolved in a mixture of chloroform (30 mL) and acetic acid (3 mL). NBS (90.6 mg, 0.50 mmol) was added to the solution and the mixture was stirred overnight in the dark. The solvents were removed on a rotary evaporator *in vacuo*. The crude product was purified by column chromatography on silica gel eluting with hexane/CH_2Cl_2 (4:1, v/v) to provide **L2**-**Br** (103 mg, 0.10 mmol, 41%) as an orange solid.

Spectral Data: ^{1}H NMR (400 MHz, $CDCl_3$): δ = 8.08−8.04 (m, 2H, Ar), 7.96 (m, 2H, Ar), 7.90−7.86 (m, 4H, Ar), 7.78−7.76 (m, 2H, Ar), 7.56−7.51 (m, 4H, Ar), 7.15 (m, 2H, Ar), 7.08 (m, 2H, Ar), 2.11 (m, 8H, C_4H_9), 1.16−1.11 (m, 8H, C_4H_9), 0.82−0.70 (m, 20H, C_4H_9) ppm. ^{13}C NMR (100 MHz, $CDCl_3$): δ = 154.34, 152.28, 151.63, 151.34, 146.61, 140.69, 140.68, 136.49, 133.53, 132.69, 130.91, 128.40, 127.97, 124.75, 123.93, 123.09, 120.52, 120.14, 119.93, 119.91, 111.13 (Ar), 55.35 (quat. C), 40.01, 26.14, 23.13, 13.89 (C_4H_9) ppm. FAB-MS (*m/z*): 1010.2 [M+1]$^+$.

2.3.3. Synthesis of *L1-TMS*

To an ice-cooled mixture of **L1**-**I** (1.09 mmol) in freshly distilled triethylamine (20 mL) and CH_2Cl_2 (20 mL) solution under nitrogen was added Pd(OAc)$_2$ (30 mg), PPh$_3$ (90 mg) and CuI (30 mg). After the solution was stirred for 30 min, trimethylsilylacetylene (0.78 mL, 5.45 mmol) was then added and the suspension was stirred for another 30 min in the ice bath before being warmed to room temperature. After reacting for 30 min at room temperature, the mixture was heated to 50 °C for 24 h. The solution was then allowed to cool to room temperature and the solvents were

removed on a rotary evaporator *in vacuo*. The crude product was purified by column chromatography on silica gel eluting with hexane/CH_2Cl_2 (1:2, v/v) to give **L1-TMS** as an orange solid in 66% yield.

Spectral Data: ^1H NMR (400 MHz, $CDCl_3$): δ = 8.02 (m, 2H, Ar), 7.83–7.80 (m, 2H, Ar), 7.77–7.75 (m, 2H, Ar), 7.69–7.67 (m, 2H, Ar), 7.64–7.61 (m, 6H, Ar), 7.52–7.50 (m, 4H, Ar), 2.05–2.01 (m, 8H, C_4H_9), 1.13–1.08 (m, 8H, C_4H_9), 0.70–0.60 (m, 20H, C_4H_9), 0.32 (s, 18H, $Si(CH_3)_3$) ppm. ^{13}C NMR (100 MHz, $CDCl_3$): δ = 194.09, 152.01, 151.02, 143.05, 142.46, 141.33, 140.28, 139.18, 135.25, 133.46, 131.29, 126.58, 125.85, 123.12, 121.02, 120.08, 120.56, 120.46, 119.79 (Ar), 84.69, 77.25 (C≡C), 55.31 (quat. C), 40.22, 25.96, 23.05, 13.85 (C_4H_9), 0.00 ($Si(CH_3)_3$) ppm. FAB-MS (*m/z*): 781.4 $[M+1]^+$.

2.3.4. Synthesis of *L2-TMS*

The similar procedure was used to prepare **L2-TMS** using **L2-Br** using hexane/CH_2Cl_2 (4:1, v/v). Orange solid. Yield: 92%.

Spectral Data: ^1H NMR (400 MHz, $CDCl_3$): δ = 8.07–8.04 (m, 2H, Ar), 7.96 (m, 2H, Ar), 7.90–7.86 (m, 4H, Ar), 7.78–7.76 (m, 2H, Ar), 7.62–7.57 (m, 4H, Ar), 7.25–7.23 (m, 4H, shielded by proton of $CHCl_3$, Ar), 2.12–2.02 (m, 8H, C_4H_9), 1.17–1.11 (m, 8H, C_4H_9), 0.80–0.70 (m, 20H, C_4H_9), 0.24 (s, 18H, $Si(CH_3)_3$) ppm. ^{13}C NMR (100 MHz, $CDCl_3$): δ = 152.29, 151.47, 146.67, 140.89, 140.75, 136.57, 133.84, 133.61, 132.80, 128.45, 128.04, 125.09, 123.98, 122.76, 122.10, 120.55, 120.28, 119.97 (Ar), 99.78, 97.90 (C≡C), 55.38 (quat. C), 40.21, 26.18, 23.18, 13.94

(C_4H_9), 0.00 (Si(CH_3)$_3$) ppm. FAB-MS (*m/z*): 1043.8 [M+1]$^+$.

2.3.5. Synthesis of L1

A mixture of **L1-TMS** (0.33 mmol) and K_2CO_3 (114 mg, 0.85 mmol) in a solution mixture of methanol (5 mL) and CH_2Cl_2 (20 mL), under a nitrogen atmosphere, was stirred at room temperature overnight. The mixture was added to CH_2Cl_2 (30 mL) washed with water (20 mL) three times and dried over anhydrous Na_2SO_4. The solvents were removed on a rotary evaporator *in vacuo*. The crude product was purified by column chromatography on silica gel eluting with hexane/CH_2Cl_2 (4:1, v/v) to afford **L1** as a yellow solid in 91% yield.

Spectral Data: ^{1}H NMR (400 MHz, CDCl$_3$): δ = 8.07−8.04 (m, 2H, Ar), 7.98 (m, 2H, Ar), 7.91 (m, 2H, Ar), 7.89−7.87 (m, 2H, Ar), 7.75−7.73 (m, 2H, Ar), 7.55−7.53 (m, 4H, Ar), 3.18 (s, 2H, C≡CH), 2.10−2.03 (m, 8H, C_4H_9), 1.17−1.12 (m, 8H, C_4H_9), 0.75−0.71 (m, 20H, C_4H_9) ppm. ^{13}C NMR (100 MHz, CDCl$_3$): δ = 154.30, 151.50, 151.30, 141.46, 140.49, 136.80, 133.52, 131.31, 128.38, 127.99, 126.64, 123.92, 120.49, 120.17, 119.90 (Ar), 84.72, 77.23 (C≡C), 55.27 (quat. C), 40.08, 26.05, 23.10, 13.85 (C_4H_9) ppm. FAB-MS (*m/z*): 736.5 [M+1]$^+$. IR (KBr) (cm^{-1}) $\nu_{(C≡C-H)}$: 3305; $\nu_{(C≡C)}$: 2105.

2.3.6.Synthesis of L2

The similar procedure was used to prepare **L2** from **L2-TMS** using hexane/CH_2Cl_2 (2:1, v/v) as eluent. Orange solid. Yield: 94%.

Spectral Data: ^{1}H NMR (400 MHz, CDCl$_3$): δ = 8.07−8.04 (m, 2H, Ar), 7.96 (m,

2H, Ar), 7.91–7.87 (m, 4H, Ar), 7.78–7.76 (m, 2H, Ar), 7.62–7.58 (m, 4H, Ar), 7.30–7.27 (m, 4H, shielded by proton of CHCl$_3$, Ar), 3.43 (s, 2H, C≡CH), 2.12–2.03 (m, 8H, C$_4$H$_9$), 1.17–1.11 (m, 8H, C$_4$H$_9$), 0.80–0.70 (m, 20H, C$_4$H$_9$) ppm. ^{13}C NMR (100 MHz, CDCl$_3$): δ = 154.31, 152.22, 151.38, 146.93, 140.91, 140.63, 136.51, 134.23, 133.52, 132.57, 128.36, 127.96, 125.10, 124.61, 123.889, 122.97, 122.66, 120.76, 120.47, 120.24, 119.90 (Ar), 81.94, 77.23 (C≡C), 55.332 (quat. C), 40.12, 26.09, 23.08, 13.84 (C$_4$H$_9$) ppm. FAB-MS (*m/z*): 900.6 [M+1]$^+$. IR (KBr) (cm^{-1}): ν$_{(C≡C-H)}$: 3306; ν$_{(C≡C)}$: 2100.

*2.3.7.Synthesis of **M1***

To a stirred mixture of **L1** (0.015 mmol) and *trans*-[Pt(PEt$_3$)$_2$PhCl] (20.1 mg, 0.030 mmol) in freshly distilled triethylamine (6 mL) and CH$_2$Cl$_2$ (6 mL) was added CuI (2.0 mg). The solution was stirred at room temperature under nitrogen over a period of 24 h. After removal of the solvent, the crude product was purified by column chromatography on silica gel eluting with hexane/CH$_2$Cl$_2$ (1:1, v/v) to furnish **M1** as an orange solid with a yield of 60%.

Spectral Data: ^{1}H NMR (400 MHz, CDCl$_3$): δ = 8.02–8.00 (m, 2H, Ar), 7.91–7.88 (m, 4H, Ar), 7.80 (d, *J* = 8.0 Hz, 2H, Ar), 7.61 (d, *J* = 8.0 Hz, 2H, Ar), 7.37–7.31 (m, 8H, Ar), 7.00–6.96 (m, 4H, Ar), 6.84–6.82 (m, 2H, Ar), 2.06–1.97 (m, 8H, C$_4$H$_9$), 1.83–1.80 (m, 24H, PC$_2$H$_5$), 1.18–1.10 (m, 44H, PC$_2$H$_5$ + C$_4$H$_9$), 0.83–0.71 (m, 20H, C$_4$H$_9$) ppm. ^{13}C NMR (100 MHz, CDCl$_3$): δ = 154.38, 151.20, 150.98, 141.55, 139.18, 137.45, 135.52, 133.54, 129.87, 128.20, 128.12, 127.80,

127.32, 125.48, 123.70, 121.27, 119.43, 119.32 (Ar), 111.05, 96.19 (C≡C), 54.86

(quat.C), 40.14, 26.05, 23.16, 15.28, 15.11, 14.94, 13.86, 8.09 (PC$_2$H$_5$ + C$_4$H$_9$) ppm.

^{31}P NMR (161 MHz, CDCl$_3$): δ = 9.67 ($^1J_{Pt-P}$ = 2622 Hz) ppm. FAB-MS (*m/z*): 1752.8

[M+1]$^+$. IR (KBr) (cm^{-1}): ν$_{(C≡C)}$: 2089.

2.3.8. Synthesis of *M2*

The similar procedure was used to prepare **M2** using **L2** eluting with

hexane/CH$_2$Cl$_2$ (1:1, v/v). Red solid. Yield: 55%.

Spectral Data: ^{1}H NMR (400 MHz, CDCl$_3$): δ = 8.06–8.03 (m, 2H, Ar),

7.95–7.90 (m, 4H, Ar), 7.85 (d, *J* = 8.0 Hz, 2H, Ar), 7.72 (d, *J* = 7.6 Hz, 2H, Ar),

7.59–7.55 (m, 4H, Ar), 7.34–7.32 (m, 4H, Ar), 7.20 (d, *J* = 3.6 Hz, 2H, Ar), 7.00–6.96

(m, 4H, Ar), 6.87 (d, *J* = 3.6 Hz, 2H, Ar), 6.83–6.80 (m, 2H, Ar), 2.12–2.03 (m, 8H,

C$_4$H$_9$), 1.80–1.74 (m, 24H, PC$_2$H$_5$), 1.16–1.08 (m, 44H, PC$_2$H$_5$ + C$_4$H$_9$), 0.80–0.70 (m,

20H, C$_4$H$_9$) ppm. ^{13}C NMR (100 MHz, CDCl$_3$): δ = 154.34, 151.98, 151.25, 141.06,

140.91, 139.56, 139.08, 136.05, 133.95, 133.52, 128.25, 128.04, 127.88, 127.36,

124.48, 123.80, 122.63, 120.25, 119.66 (Ar), 119.59, 101.3 (C≡C), 55.21 (quat. C),

40.20, 26.08, 23.13, 15.30, 15.13, 14.96, 13.86, 8.07 (PC$_2$H$_5$ + C$_4$H$_9$) ppm. ^{31}P NMR

(161 MHz, CDCl$_3$): δ = 10.03 (J_{Pt-P} = 2612 Hz) ppm. MALDI-TOF: *m/z* calcd for

C$_{96}$H$_{124}$N$_2$P$_4$Pt$_2$S$_3$: 1915.7183; found: 1915.8225. IR (KBr) (cm^{-1}): ν$_{(C≡C)}$: 2081.

2.3.9. Synthesis of *P1*

To a stirred mixture of **L1** (0.10 mmol) and *trans*-[Pt(PBu$_3$)$_2$Cl$_2$] (67.0 mg, 0.10 mmol) in freshly distilled triethylamine (20 mL) and CH$_2$Cl$_2$ (20 mL) solution was added CuI (5 mg). The solution was stirred at room temperature for 24 h under a nitrogen atmosphere. The solvents were removed on a rotary evaporator *in vacuo*. The residue was redissolved in CH$_2$Cl$_2$ and filtered through a short aluminium oxide column using the same eluent to remove ionic impurities and catalyst residue. After removal of the solvent, the crude product was washed with hexane three times followed by methanol three times and then repeated precipitation from CH$_2$Cl$_2$/methanol and drying *in vacuo* to afford polymer **P1** as an orange solid in 53% yield.

Spectral Data: ^{1}H NMR (400 MHz, CDCl$_3$): δ = 8.03 (m, 2H, Ar), 7.92–7.80 (m, 6H, Ar), 7.64–7.62 (m, 2H, Ar), 7.31–7.26 (m, 4H, Ar), 2.24 (m, 12H, PC$_4$H$_9$), 1.70 (m, 12H, PC$_4$H$_9$), 1.56–1.50 (m, 20H, shielded by proton of H$_2$O, C$_4$H$_9$ + PC$_4$H$_9$), 1.13 (m, 8H, C$_4$H$_9$), 0.99–0.96 (m, 24H, C$_4$H$_9$ + PC$_4$H$_9$), 0.74 (m, 18H, PC$_4$H$_9$) ppm. ^{31}P NMR (161 MHz, CDCl$_3$): δ = 2.93 ($^1J_{P–Pt}$ = 2341 Hz) ppm. IR (KBr) (cm^{-1}): ν$_{(C≡C)}$: 2092.

2.3.10. Synthesis of P2

The similar procedure was used to prepare **P2** using **L2**. Reddish-orange solid. Yield: 56%. *Spectral Data*: ^{1}H NMR (400 MHz, CDCl$_3$): δ = 8.06–8.04 (m, 2H, Ar), 7.95–7.85 (m, 6H, Ar), 7.75–7.73 (m, 4H, Ar), 7.22 (m, 2H, Ar), 6.87 (m, 2H, Ar), 2.19–2.04 (m, 20H, C$_4$H$_9$ + PC$_4$H$_9$), 1.67–1.49 (m, 24H, shielded by the proton of

H$_2$O, C$_4$H$_9$ + PC$_4$H$_9$), 1.17–1.12 (m, 8H, C$_4$H$_9$), 1.01–0.96 (m, 18H, PC$_4$H$_9$), 0.79–0.71 (m, 20H, C$_4$H$_9$ + PC$_4$H$_9$) ppm. ^{31}P NMR (161 MHz, CDCl$_3$): δ = 3.37 ($^1J_{P–Pt}$ = 2314 Hz) ppm. IR (KBr) (cm^{-1}): ν$_{(C≡C)}$: 2087.

3. Results and discussion

3.1. Synthesis and structural characterization

The synthetic strategies to **M1−M2** and **P1−P2** are shown in Scheme 1. By the Stiile coupling of 2,7-dibromo-2,1,3-benzothiadiazole and tributyl(9,9-dibutyl-fluoren-2-yl)stannane, 4,7-bis(9,9-dibutylfluoren-2-yl)-2,1,3-benzothiadiazole (**2**) can be obtained in good yield. Iodination of **2** with I$_2$ afforded **L1-I** which underwent another Stille couping reaction with tributyl(thiophen-2-yl)stannane to give 4,7-bis(7-(thiophen-2-yl)-9,9-dibutylfluoren-2-yl)-2,1,3-benzothiadiazole (**3**). Bromination of **3** with NBS led to **L2-Br**. By Sonogashira coupling reaction, the bromide or iodide groups were converted into the corresponding trimethylsilylethynyl (TMS) groups in a CH$_2$Cl$_2$/NEt$_3$ mixture using CuI, Pd(OAc)$_2$ and PPh$_3$ as the catalyst medium [31]. By following desilylation with potassium carbonate in methanol, the diethynyl ligands **L1** and **L2** were obtained as yellow to orange solids. Polymers **P1−P2** and their model compounds **M1−M2** were prepared by the Sonogashira-type dehydrohalogenation between each of the diethynyl precursors (**L1** or **L2**) and the corresponding platinum precursors trans-Pt(PBu$_3$)$_2$Cl$_2$ and trans-Pt(PEt$_3$)$_2$(Ph)Cl with the stoichiometric ratio of 1:1 and 1:2, respectively [32]. Polymers **P1−P2** were

purified by flash column chromatography over neutral Al_2O_3 to remove ionic impurities and catalyst residues, and repeated precipitation and isolation and obtained as orange to red-orange solids.
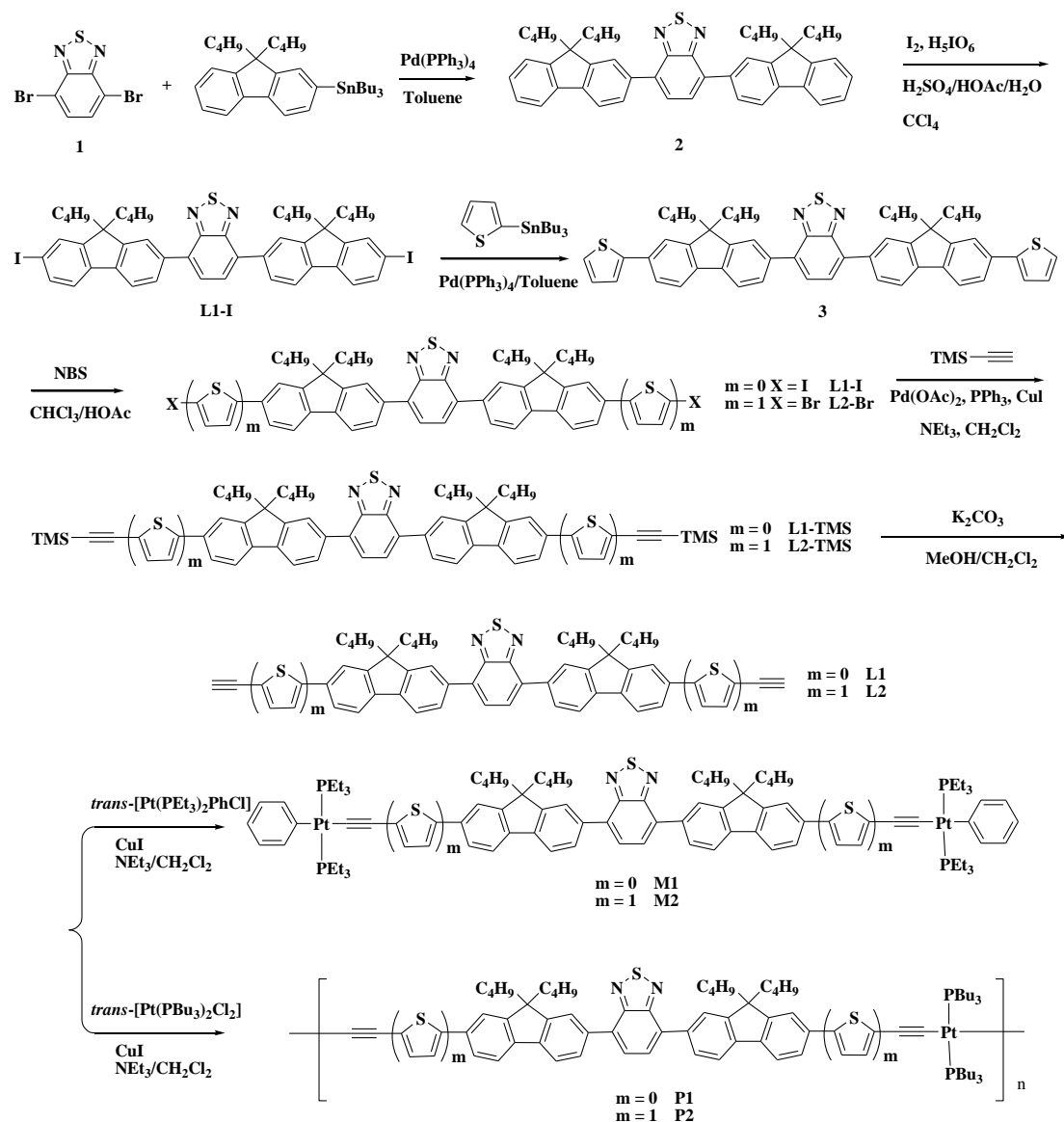

Scheme 1. The synthetic pathways of **P1−P2** and **M1−M2**.

Model compounds **M1−M2** and platinum(II) polymers **P1−P2** were fully characterized by common spectroscopic techniques including infrared (IR) and NMR (^1H, ^{13}C and ^{31}P) spectroscopies, and FAB mass spectrometry (for model compounds).

The strong single ^{31}P signal flanked with two satellites for Pt(II) polymers and model compounds is in agreement with a *trans*-geometry of the Pt(PBu$_3$)$_2$ and Pt(PEt$_3$)$_2$Ph units in a square-planar geometry. Saliently, the $^1J_{\text{P-Pt}}$ values of 2314−2341 Hz for the PBu$_3$ moieties and 2612−2622 Hz for the PEt$_3$ moieties are typical of those for the related *trans*-PtP$_2$ alkynyl systems, which are smaller than those of the *cis*-isomers (> 3500 Hz) [33]. The FT-IR spectra indicate that the v(C≡C) stretching frequencies of **P1−P2** are located at 2087−2092 cm^{-1} and **M1−M2** at 2081−2089 cm^{-1}, which are lower than those for the terminal acetylenic C≡C−H stretching vibrations at 2100−2105 cm^{-1}. It may be ascribed to either the metal-to-alkyne π back bonding or the M$^{\delta+}$−C$^{\delta-}$ polarity which contributes to a higher degree of conjugation in the former case [32]. From the crystal structures of **L1-TMS** and **3** shown in Figs. 2 and 3, respectively, it is clear that the three benzothiadiazole and dibutylfluorene rings are not fully coplanar with each other in each case, with notable twists between them. The respective dihedral angles are 36.98 and 40.03° for **L1-TMS** and 42.32 and 35.62° for **3**. For **3**, the thiophene rings are almost coplanar with the adjacent fluorenyl rings, ensuring a greater degree of π-conjugation.

Molecular weights and polydispersity indices (PDIs) of the polymers were determined by gel permeation chromatography (GPC) analysis with a polystyrene standard calibration. The GPC results are summarized in Table 1. **P1** exhibits a high weight-average molecular weight (M_w) of 105.9 kg/mol with a PDI of 1.43. The other polymer **P2** has a lower M_w of 41.5 kg/mol with a PDI of 1.35. The difference of the molecular weights may be resulted from the reactivity and steric hindrance of the

donor segments as well as solubility of ligands. While GPC does not give absolute values of molecular weights but provides a measure of hydrodynamic volume, there is probably notable differences in the hydrodynamic behavior of rigid-rod type polymers in solution from those for flexible polymers. So, we would anticipate an overestimation of molecular weights, leading to certain systematic errors in the GPC measurements.
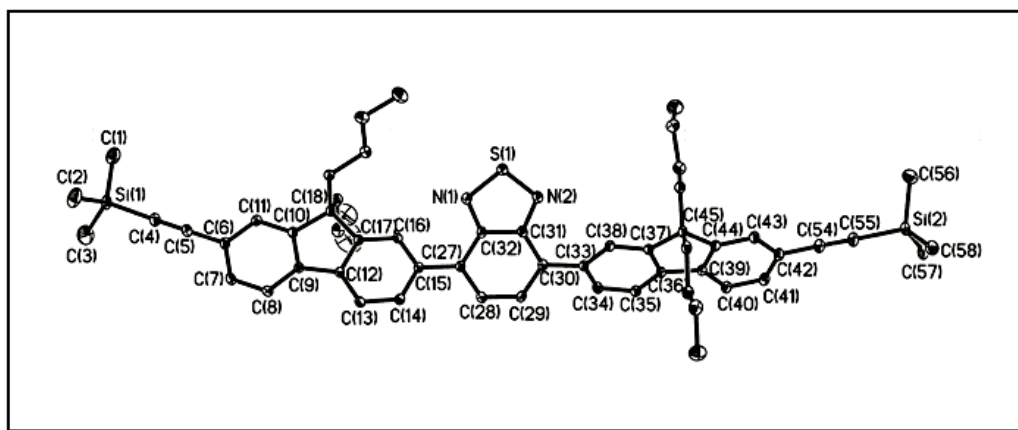
Fig. 2. Molecular structure of **L1-TMS**, with the thermal ellipsoids shown at the 25% probability level. All hydrogen atoms are omitted for clarity.
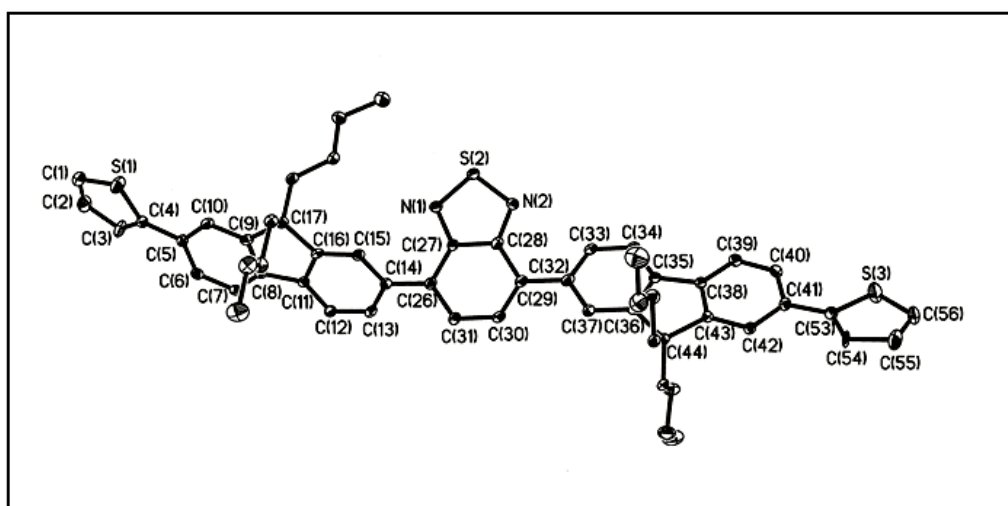
Fig. 3. Molecular structure of **3**, with the thermal ellipsoids shown at the 25% probability level. All hydrogen atoms are omitted for clarity.

19

3.2. Thermal, photophysical and electrochemical properties

Thermal gravimetric analysis (TGA) data under nitrogen show that polymers **P1−P2** exhibit good thermal stability with onset decomposition temperatures (T_{dec}) at 311 and 350 °C, respectively (Table 1), and the respective percent weight loss indicates the removal of one PBu$_3$ and some of the Bu groups from their polymers in the decomposition step. Decomposition onset was defined by a 5 wt.-% loss in each case. These values are appreciably higher than those for the polymers with dithienyl (278 °C) [34] and bis(thienyl)benzothiadiazole (284 °C) [35] moieties. This level of thermal stability is adequate to meet the requirement of optoelectronic device engineering.

The photophysical properties of all new diethynyl ligands and their metal complexes were investigated by UV/Vis and photoluminescence (PL) spectroscopies in CH$_2$Cl$_2$ solution (Table 2). The UV/Vis absorption and PL emission spectra of **M1** and **P1** are shown in Fig. 4, and those of **M2** and **P2** are shown in Fig. 5. Both **L1** and **L2** show two strong absorptions (328, 413 nm for **L1** and 353, 425 nm for **L2**), which are assigned to the electronic transitions in the fluorene-benzothiadiazole system. The small red shift of absorption peaks of **L2** relative to **L1** is due to the presence of additional thiophene rings, which extends the π-conjugation of **L2** as compared to that of **L1**. All of the Pt compounds were also characterized by two major bands in the absorption spectra. As compared to the free alkynes, there is a clear red shift in the absorption wavelength for their corresponding platinum compounds which suggests

π-conjugation through the metal centre due to the dπ-pπ interactions between Pt ion and alkyne ligands. The effect of central spacer group R on the color and bandgap in these polyplatinaynes can be rationalized in Table 3 [34−36]. Typical of many D-A conjugated polymers, alternating thiophene (D) and benzothiadiazole (A) groups in the segment can narrow down the E_g significantly (rows 1−3). The higher bandgap property of **P1** (2.42 eV, row 4) relative to the Pt-polyyne with bis(thiophenyl)benzothiadiazole (1.85 eV, row 3, [35]) is attributed to the twisted configuration of the individual aryl rings in the segment. In other words, the weakly electron-donating fluorenyl ring is shown to be less effective than the strongly-donating thiophenyl ring in conjugating with the electron-accepting benzothiadiazole unit, which causes a less significant intramolecular charge transfer even in the ground state. The extent of π-conjugation for the polymer with R = benzothiadiazole (E_g = 2.20 eV, row 2, [36]) is even stronger than that for **P1** (row 4). As expected, the HOMO-LUMO gap of **P1** (or **M1**) can be notably reduced by introducing the electron-rich thiophene ring to the spacer in **P2** (or **M2**), although the reduction is not that remarkable.

All of the platinum complexes show red emission bands in CH_2Cl_2 solution at room temperature (Table 2, Figs. 4 and 5). In general, red luminescent polymers usually show a low emission efficiency since red chromophores are prone to aggregation in the solid state and are highly susceptible to concentration quenching [37, 38]. At 293 K, **P1** shows an emission peak at 595 nm with the lifetime of 2.04 ns in dilute solution whereas polymer **P2** emits at 611 nm with the lifetime of 1.11 ns. In

both cases, no triplet emission was observed which manifests to the energy gap law for low-gap polyplatinaynes [39]. Besides, as reported in the literature [34, 40], the extended heteroaryl ring in the ligand chromophore greatly reduces the heavy metal effect in **P1** and **P2** which is mainly responsible for facilitating the intersystem crossing and hence phosphorescence emission. So, the ligand-dominating singlet excited state instead of the triplet state should contribute to the photoinduced charge separation in the energy conversion for both polymers. The photoluminescence quantum yields (Φ) of the polymers **P1−P2** are generally lower than those for **M1−M2** [39]. All of the Pt compounds undergo a rigidochromic blue shift in the emission wavelength upon cooling of their solutions to 77 K. The hypsochromic shift observed at low temperature is mainly caused by the solvent reorganization in a fluid solution at 77 K that can readily stabilize the charge transfer states prior to emission [41]. This process is significantly impeded in a rigid matrix at 77 K, and hence fluorescence appears at a higher energy. The absence of vibronic progression in the emission profile (both at 293 and 77 K) suggests mostly a charge-transfer state but not the ligand-centered π-π* excited state. The observed emission lifetimes (τ) of our platinum compounds at 77 K are longer than those measured at room temperature. In these systems, the τ values are generally determined by nonradiative decay rates which usually decreases as temperature decreases. Thus, a lengthening of τ at a low temperature would be expected [42].
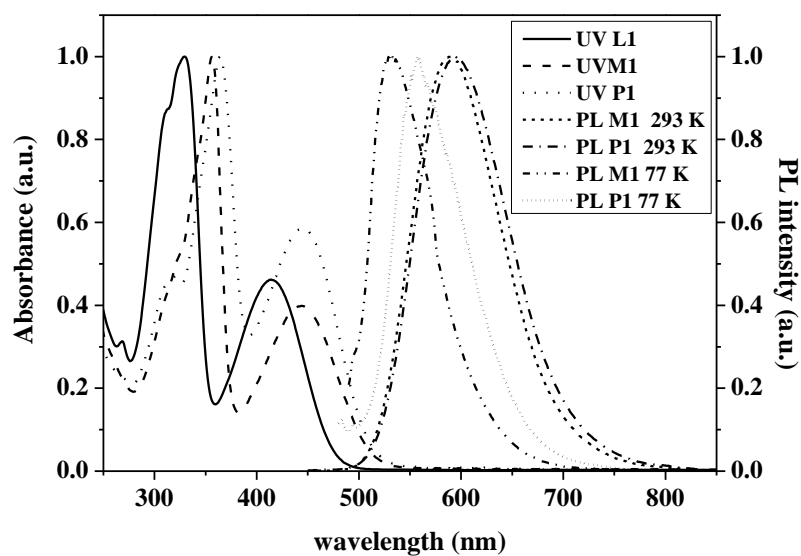
**Fig. 4.** Normalized absorption and emission spectra of **L1**, **M1** and **P1** in CH₂Cl₂ solution at 293 K and 77 K.
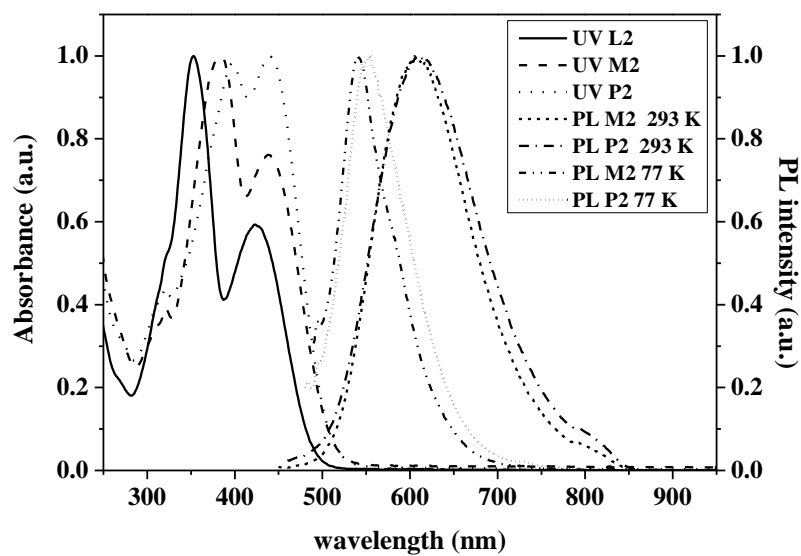
Fig. 5. Normalized absorption and emission spectra of **L2**, **M2** and **P2** in CH₂Cl₂ solution at 293 K and 77 K.

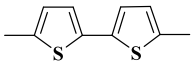**Table 1.** GPC and TGA results of **P1−P2**.

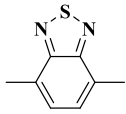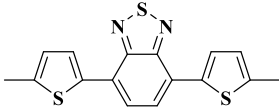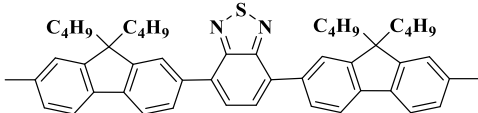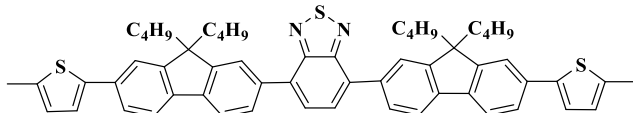| Polymer	M_n[a]	M_w[b]	PDI[c]	DP[d]	T_{dec} [°C]
P1	74040	105940	1.43	55	311
P2	30785	41450	1.35	21	350

[a] M_n = Number-average molecular weight

[b] M_w = Weight-average molecular weight

[c] PDI = Polydispersity index

[d] DP = Degree of polymerization (calculated from M_n values)

Table 2. Photophysical data of all the platinum(II) complexes.

	Absorption (293 K)		Emission (293 K)			Emission (77 K)	
	λ_{abs} [nm] CH_2Cl_2[a]	Bandgap E_g [eV][b]	λ_{em} [nm] CH_2Cl_2	Φ (%)	τ_P (ns)	λ_{em} [nm] CH_2Cl_2	τ_P (ns)
M1	355 (10.2), 445 (3.8)	2.42	588	7.5	3.69	531	3.88
M2	384 (8.3), 439 (6.3)	2.36	605	9.1	2.51	540	2.67
P1	363, 447	2.42	595	2.2	2.04	559	2.70
P2	396, 441	2.40	611	4.3	1.11	555	1.37

Table 3. Variation of E_g values with central spacer group R in polyplatinaynes.
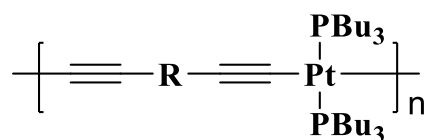
R	E_g (eV)	Color	Ref.
	2.55	Yellow	[34]

	2.20	Red	[36]
	1.85	Dark purple	[35]
	2.42	Orange	This work
	2.40	Red-orange	This work

The HOMO and LUMO levels of the polymers **P1**–**P2** were calculated based on the redox potentials determined from electrochemical measurements using cyclic voltammetry. The key data are gathered in Table 4. From the onset values of oxidation potential ($E_{onset, ox}$), the HOMO levels of the polymers were calculated according to the equation $E_{HOMO} = -(E_{onset, ox} + 4.72)$ eV where the unit of potential is V versus Ag/AgCl) while the LUMO levels were determined from the optical bandgap and the energy level of HOMO using the equation $E_{LUMO} = (E_{HOMO} + E_g^{opt})$ eV [43, 44]. **P1** shows an irreversible oxidation wave at 1.11 eV while **P2** shows a similar oxidation wave at 0.99 eV. Both of them can be attributed to the oxidation of fluorene ring. It is also found that introduction of thiophene rings would elevate the HOMO level in **P2** (-5.71 eV) relative to **P1** (−5.83 eV), indicating that **P2** is more electropositive (or has a lower ionization potential) than **P1**, and hence a better hole transport ability in **P2** would be anticipated.

Table 4. Electrochemical data of platinum(II) polymers **P1**−**P2**

Polymer	Oxidation potential (V)	Energy levels (eV)		Bandgap (eV)
	$E_{onset, ox}$ [a]	E_{HOMO} [b]	E_{LUMO} [c]	E_g^{opt} [d]
P1	+1.11	−5.83	−3.41	2.42
P2	+0.99	−5.71	−3.31	2.40

[a] $E_{onset, ox}$ are the onset potentials of oxidation

[b] $E_{HOMO} = -(E_{onset, ox} + 4.72)$ eV

[c] Calculated from the optical bandgap and the energy level of HOMO and $E_{LUMO} = (E_{HOMO} + E_g^{opt})$ eV

[d] E_g^{opt} = Optical bandgap as estimated from the absorption onset in the solution state ($E_g^{opt} = 1240/\lambda_{abs}^{onset}$ eV).

4.   Conclusion

In summary, we have synthesized two stable and soluble red-emitting platinum-acetylide organometallic polymers with dibutylfluorene and 2,1,3-benzothiadiazole as the central core components and their photophysical properties were studied. The addition of less electron-donating fluorenyl rings to a strongly electron-accepting benzothiadiazole cannot extend the π-conjugation effectively which is correlated to the twisting of the aryl rings in the solid state. The structure-bandgap relationships and control of bandgap of these polyplatinaynes are rationalized in terms of the structural feature of the central aromatic segment. This provides valuable insight to the future design of new photofunctional polymers for optoelectronic applications.

Acknowledgements

References

[1] Electronic Materials: The Oligomer Approach (Eds. K. Müllen, G. Wegner), Wiley-VCH, 1998.

[2] Design and Synthesis of Conjugated Polymers (Eds. M. Leclerc, J.-F. Morin), Wiley-VCH, 2010.

[3] Z.Y. Wang, Near-infrared Organic Materials and Emerging Applications. Taylor & Francis Group, LLC, Boca Raton 2013.

[4] G. Qian G, Z.Y. Wang, Chem. Asian J. 5 (2010) 1006–1029.

[5] H.F. Xiang, J.H. Chen, X.F. Ma, X.F. Zhou, J.J. Chruma. Chem. Soc. Rev. 42 (2013) 6128–6185.

[6] Y. Zhang, X. Bao, M. Xiao, H. Tan, Q. Tao, Y. Wang, Y. Liu, R. Yang, W. Zhu, J. Mater. Chem. A 3 (2015) 886–893.

[7] T. Liu, L. Zhu, S. Gong, C. Zhong, G. Xie, E. Mao, J. Fang, D. Ma, C. Yang, Adv. Optical Mater. 5 (2017) 1700145.

[8] M. Wang, X. Hu, P. Liu, W. Li, X. Gong, F. Huang, Y. Cao, J. Am. Chem. Soc. 133 (2011) 9638–9641.

[9] X. Guo, H. Xin, F.S. Kim, A.D.T. Liyanage, S.A. Jenekhe, M.D. Watson, Macromolecules 44 (2011) 269–277.

[10] Y.J. Cheng, S.H. Yang, C.S. Hsu, Chem. Rev. 109 (2009) 5868–5923.

[11] X. Guo, A. Facchetti, T.J. Marks. Chem. Rev. 114 (2014) 8943–9021.

[12] Y.F. Li, Acc. Chem. Res. 45 (2011) 723–733.

[13] T. Lei, J.Y. Wang, J. Pei, Acc. Chem. Res. 47 (2014) 1117–1126.

[14] T.C. Parker, D.G. Patel, K. Moudgil, S. Barlow, C. Risko, J.L. Brédas, J.R. Reynolds, S.R. Marder, Mater. Horizon. 2 (2015) 22–36.

[15] M. Zhang, H.N. Tsao, W. Pisula, C. Yang, A. Mishra, K. Müllen, J. Am. Chem. Soc. 129 (2007) 3472–3473.

[16] E. Zhou, J. Cong, S. Yamakawa, Q. Wei, M. Nakamura, K. Tajima, C. Yang, K. Hashimoto, Macromolecules 43 (2010) 2873–2879.

[17] B.A.D. Neto, A.A.M. Lapis, E.N. da Silva Júnior, J. Dupont, Eur. J. Org. Chem. 2013 (2013) 228–255.

[18] Y. Zhang, J. Song, J. Qu, P.-C. Qian, W.-Y. Wong, Sci. China Chem. 64 (2021) 341–357.

[19] J. Liu, Q.G. Zhou, Y.X. Cheng, Y.H. Geng, L.X. Wang, D.G. Ma, X.B. Jing, F.S. Wang, Adv. Funct. Mater. 16 (2006) 957–965.

[20] L. Chen, P. Li, Y. Cheng, Z. Xie, L.Wang, X. Jing, F. Wang, Adv. Mater. 23 (2011) 2986–2990.

[21] J. Liu, L. Chen, S. Shao, Z. Xie, Y. Cheng, Y. Geng, L. Wang, X. Jing, F. Wang J. Mater. Chem. 18 (2008) 319–327.

[22] S.Y. Ku, L.C. Chi, W.Y. Hung, S.W. Yang, T.C. Tsai, K.T. Wong, Y.H. Chen, C.I. Wu, J. Mater. Chem. 19 (2009) 773–780.

[23] J. Zhang, W. Chen, A.J. Rojas, E.V. Jucov, T.V. Timofeeva, T.C. Parker, S. Barlow, S.R. Marder, J. Am. Chem. Soc. 135 (2013) 16376–16379.

[24] P. Herguth, X. Jiang, M.S. Liu, A.K.-Y. Jen, Macromolecules 35 (2002) 6094-6099.

[25] A.C. Arias, J.D. MacKenzie, R. Stevenson, J.J. Halls, M. Inbasekaran, E.P. Woo, D. Richards, R.H. Friend, Macromolecules 34 (2001) 6005–6013.

[26] G. W. Parshall, Inorg. Synth. 12 (1970) 26–33.

[27] G. B. Kauffman, L. A. Teterm, Inorg. Synth. 7 (1963) 245–249.

[28] SAINT, Reference manual, Siemens Energy and Automation, Madison, Madison, WI, 1994−1996.

[29] G. M. Sheldrick, SADABS, Empirical Absorption Correction Program, University of Göttingen, 1997.

[30] C. Qin, Y. Fu, C.-H. Chui, C.-W. Kan, Z. Xie, L. Wang, W.-Y. Wong, Macromol. Rapid Commun. 32 (2011) 1472-1477.

[31] A. Haque, R.A. Al-Balushi, I.J. Al-Busaidi, M.S. Khan, P.R. Raithby, Chem. Rev. 118 (2018) 8474-8597.

[32] J. Lewis, N.J. Long, P.R. Raithby, G.P. Shields, W.-Y. Wong, M. Younus, J. Chem. Soc., Dalton Trans. (1997) 4283-4288.

[33] S.O. Grim, R.L. Keiter, W. McFarlane, Inorg. Chem. 6 (1967) 1133–1137.

[34] N. Chawdhury, A. Kohler, R.H. Friend, W.-Y. Wong, J. Lewis, M. Younus, P.R. Raithby, T.C. Corcoran, M.R.A. Al-Mandhary, M.S. Khan, J. Chem. Phys. 110 (1999) 4963–4970.

[35] W.-Y. Wong, X.-Z. Wang, Z. He, A.B. Djurišić, C.-T. Yip, K.-Y. Cheung, H. Wang, C.S.K. Mak, W.-K. Chan, Nat. Mater. 6 (2007) 521–527.

[36] J.S. Wilson, A. Köhler, R.H. Friend, M.K. Al-Suti, M.R.A. Al-Mandhary, M.S. Khan, P.R. Raithby, J. Chem. Phys. 113 (2000) 7627–7634.

[37] C.-T. Chen, Chem. Mater. 16 (2004) 4389–4400.

[38] S. D. Cummings, R. Eisenberg, J. Am. Chem. Soc. 118 (1996) 1949–1960.

[39] J. S. Wilson, N. Chawdhury, M. R. A. Al-Mandhary, M. Younus, M. S. Khan, P. R. Raithby, A. Köhler, R. H. Friend, J. Am. Chem. Soc. 123 (2001) 9412–9417.

[40] M. An, X. Yan, Z. Tian, J. Zhao, B. Liu, F. Dang, X. Yang, Y. Wu, G. Zhou, Y. Ren, L. Gao, J. Mater. Chem. C 4 (2016) 5626–5633.

[41] A. B. Tamayo, S. Garon, T. Sajoto, P. I. Djurovich, I. M. Tsyba, R. Bau, M. E. Thompson, Inorg. Chem. 44 (2005) 8723–8732.

[42] C.-L. Ho, W.-Y. Wong, G.-J. Zhou, B. Yao, Z. Xie, L. Wang, Adv. Funct. Mater. 17 (2007) 2925–2936.

[43] J. Hou, Z. Tan, Y. Yan, Y. He, C. Yang, Y. Li, J. Am. Chem. Soc. 128 (2006) 4911–4916.

[44] C. G. Van de Walle, J. Neugebauer, Nature 423 (2003) 626–628.